Variability of the Oceanic Mixed Layer 1960-2004

James A. Carton, Semyon A. Grodsky, and Hailong Liu

November 30, 2006

April 9, 2007

Revised for the Journal of Climate

Department of Atmospheric and Oceanic Science
University of Maryland, College Park, MD 20742

Corresponding author:
senya@atmos.umd.edu

ABSTRACT

A new monthly uniformly gridded analysis of mixed layer properties based on the World Ocean Atlas 2005 global ocean data set is used to examine interannual and longer changes in mixed layer properties during the 45-year period 1960-2004. The analysis reveals substantial variability in the winter-spring depth of the mixed layer in the subtropics and midlatitudes. In the North Pacific an Empirical Orthogonal Eigenfunction analysis shows a pattern of mixed layer depth variability peaking in the central subtropics. This pattern occurs coincident with intensification of local surface winds and may be responsible for the SST changes associated with the Pacific Decadal Oscillation. Years with deep winter-spring mixed layers coincide with years in which winter-spring SST is low. In the North Atlantic a pattern of winter-spring mixed layer depth variability occurs that is not so obviously connected to local changes in winds or SST, suggesting that other processes such as advection are more important. Interestingly, at decadal periods the winter-spring mixed layers of both basins show trends, deepening by 10-40m over the 45-year period of this analysis. The long term mixed layer deepening is even stronger (50-100m) in the North Atlantic subpolar gyre. At tropical latitudes the boreal winter mixed layer varies in phase with the Southern Oscillation Index, deepening in the eastern Pacific and shallowing in the western Pacific and eastern Indian Oceans during El Niños. In boreal summer the mixed layer in the Arabian Sea region of the western Indian Ocean varies in response to changes in the strength of the Southwest Monsoon.

1. Introduction

The oceanic mixed layer provides a connection between atmosphere and ocean and thus plays a central role in climate variability. For example, recent studies suggest that changes in the maximum depth of the mixed layer from one winter to the next may explain the reemergence of sea surface temperature (SST) anomalies and thus persistence of wintertime SST patterns (*Timlin et al., 2002; Deser et al., 2003).* Here we exploit the availability of a newly expanded archive of profile observations to determine the spatial and temporal structure of mixed layer depth variability during the 45-year period 1960-2004. Our goal is to document these changes to the extent possible given the limitations of the historical observational record.

In the extratropics mixed layers undergo large seasonal depth variations as a result of seasonally varying balances in the mixed layer heat and salt budgets. Summer conditions of high sunlight and mild winds produce shallow, strongly stratified mixed layers. The maximum mixed layer depths (MLDs), in excess of 100m at 40^{o}N, occur in winter and early spring as the result of reductions in surface buoyancy flux and increases in turbulent mixing (e.g. *Monterey and Levitus*, 1997; *Kara et al*., 2002; and *de Boyer Montegut et al.*, 2004).

A number of studies have examined mixed layer dynamics at fixed mooring sites such as the *Freeland et al. (1997)* examination of Ocean Station Papa (50^{o}N, 145^{o}W) in the North Pacific. These examinations reveal the presence of substantial subseasonal (interannual and longer) variations of MLD. At Ocean Station Papa, *Freeland et al.* found 10-20m year-to-year depth variations as well as a long-term 6 m decade^{-1} shallowing trend. These subseasonal variations are linked to the seasonal cycle because they result from terms in the heat and salt balances of the mixed layer that are important when the mixed layer is deepening. The variations are masked by the appearance of shallow mixed layers in summer.

In addition to understanding temporal variations of MLD we would like to explore their spatial structure. For the North Pacific winter-spring mixed layer *Polovina et al.* (1995*)* examined the historical profile data set for the years 1977-1988 relative to 1960-1976 looking for evidence of a 'climate transition'. In contrast to the shallowing trend noted at ocean station Papa, they found a 30-80% deepening in MLD in the subtropics between these two time periods. The authors ascribe this dramatic change to the deepening of the Aleutian low pressure system and the consequent intensification of surface winds.

Indeed, since 1960 meteorological conditions in the subtropical North Pacific do appear to have undergone a transition (*Bond et al.,* 2003). The period prior to the mid-1970s is characterized by winters with warm subtropical SSTs, cool eastern tropical SSTs, weakened midlatitude westerly winds and Aleutian low pressure system (the negative phase of the Pacific Decadal Oscillation, PDO) (*Mantua et al.*, 1997). More recent decades are characterized by conditions where these anomalies are reversed (the positive phase of the PDO). Incidentally, the transition seems to have induced corresponding changes in the ecosystem of the North Pacific because of the impact of changing MLD on nutrient supply to the mixed layer (*Polovina et al.,* 1995*; Chavez et al.,* 2003; *Chai et al.*, 2003). Studies of the anomaly mixed layer heat balance in this region (see *e.g. Alexander et al*., 2002; *Qu,* 2003) indicate the importance of forcing by surface heat flux, while Ekman transport acts to dampen temperature anomalies.

Like the North Pacific, the wintertime climate of the subtropical-to-subpolar North Atlantic is also subject to decadal variability. Since the 1960s this region has experienced a gradual increase in the latitude and strength of wintertime storms as reflected in an increasing value of the North Atlantic Oscillation (NAO) Index (*Hurrell, 1995*). These decades have also seen a warming of SST and rising upper ocean heat storage in the subtropical gyre and cooling

and freshening in the subpolar gyre (*Dickson et al., 2000; Flatau et al., 2001; Curry et al., 2003; Boyer et al., 2005; Levitus et al., 2005*).

One subtropical Atlantic location where the decadal trends of mixed layer properties have been explored is at Hydrostation S (32^{o}N, 64^{o}W) in the Sargasso Sea. There *Michaels and Knap (1996)* reviewed historical mixed layer properties from 1955 through 1994 relying mainly on bottle data and found quasi-decadal timescale variations and variations with periods longer than the Hydrostation S record. In late 1950s through 1960s the time-series show winter MLDs of 200-450 m. After 1970, the mixing is shallower (100-300m), with short periods of deeper MLDs. Our own re-examination of the Hydrostation S bottle data shows that the winter MLD deepened since 1990. So, the linear trend of winter MLD over the whole period 1960-2005 is quite weak. Before 1980, interannual deepening events of winter MLD at the Hydrostation S were found to be correlated with the El Niño events in the Pacific, but this correspondence is less evident in the records after 1980. The relationship to SST was explored by *Bates (2001)* who found negative relationship (r=-0.56) for MLD/SST correlation.

The most dramatic changes of the mixed layer occur in the North Atlantic subpolar gyre. At the Ocean Weather Station Bravo in the Labrador Sea the upper and intermediate layers have cooled and freshened during the past 3–4 decades causing deeper mixed layers. These changes have apparently been caused by the changes in storminess associated with the rising NAO Index (*Dickson et al*., 2002). At the station M at 66N, 2E in the Norwegian Sea, in contrast, the winter MLD has no significant long term trend. At this eastern North Atlantic location outside the subpolar gyre the mixed layer cannot penetrate through the base of the nearsurface water mass known as Atlantic Water (~300m), and thus here MLD variability is mostly governed by horizontal advection rather than surface forcing (*Nilsen* and *Falck*, 2006).

Low frequency changes in MLD in the tropics are somewhat different than those at higher latitudes. *Wang and McPhaden* (2000) and *Cronin and Kessler* (2002) both examine the moored time series at 110^{o}W in the eastern equatorial Pacific and show that increases in MLD are associated with *decreases* in winds and *increases* in SST, rather than the reverse. In an analysis of observations since 1992 *Lorbacher et al.* (2006) examine the spatial structure of MLD variations associated with the 1997 El Niño and show an out of phase relationship between changes in MLD in the eastern and western equatorial Pacific (see their Fig. 16).

In this study we take an advantage of the 7.9 million stations contained in the newly available World Ocean Database 2005 (*Boyer et al., 2006*) as well as recent work on mixed layer estimation by *de Boyer Montegut et al.* (2004) to reexamine the geographic and temporal variability of mixed layer properties during the 45-year period 1960-2004. We begin with a brief comparison to the alternative analysis of *White (1995)* and an examination of the impact of limitations in the salinity profile database on data coverage. The remainder of the paper examines interannual and decadal variability in the northern hemisphere and tropical mixed layer and the relationship between subseasonal changes in MLD, winds, and SST.

2. Data and Methods

The estimates of mixed layer properties presented here are based on the combined set of temperature and salinity vertical profiles from all available instruments contained in the World Ocean Database 2005 archive for the period 1960 through 2004. We use data from the mechanical bathythermographs (MBT), expendable bathythermographs (XBT), conductivity-temperature-depth casts (CTD), as well ocean station data (OSD), moored buoys (MRB), and drifting buoys (DRB). The final four years of the database contain an increasing number of

profiles from the new ARGO system (PFL), causing the amount of salinity information to increase dramatically. This approach (based on individual vertical profiles) minimizes possible dependence of the results on biases in temperature and salinity if these biases are depth independent for each profile.

Many different criteria have been suggested in the literature for determining the depth of the base of the mixed layer (see *de Boyer Montegut et al., 2004;* and *Lorbacher et al., 2006* for recent discussions). Here we generally follow the methodology of *de Boyer Montegut et al. (2004)* who define this depth for each profile based on the temperature- or density-difference from the temperature or density at a reference depth of 10 m. This reference depth was shown to be sufficiently deep to avoid aliasing by the diurnal signal, but shallow enough to give a reasonable approximation of monthly SST.

Our temperature-based criterion defines MLD as the depth at which temperature changes by $|\Delta T| = 0.2^{o}$C relative to its value at 10m depth. The 0.2^{o}C value is chosen following *de Boyer Montegut et al. (2004)* partly as a compromise between the need to account for accuracy of MLD retrieval and the need to avoid sensitivity of the results to measurement error. Here we define the depth of the mixed layer by the *absolute difference* of temperature, $|\Delta T|$, rather than only the *negative difference* of temperature to account fro mixed layers with of temperature inversions in salt-stratified situations (most common at high latitudes. See Appendix). For comparison, an alternative analysis by *White (1995),* uses a reference level of 0 m and a larger $\Delta T = 1^{o}$C temperature criterion.

In addition to a temperature-based estimate of MLD, if profiles include both temperature and salinity (approximately 25% of all casts), we may also compute a density-based MLD estimate. The increase in density, $\Delta\sigma$, which defines the depth of the base of the mixed layer is

chosen, following the variable density criterion of *Monterey and Levitus* (1997), to be locally compatible with the temperature-based estimates (that is, $\Delta\sigma = \partial\sigma / \partial T \times 0.2^{o} C$). This study relies primarily on temperature-based estimates because of their superior spatial and temporal coverage (unless specified, the acronym MLD, standing for mixed layer depth, will refer to the temperature-based estimates exclusively). The differences between the two estimates are briefly discussed in Section 3.

In our processing we have eliminated all profiles if flagged by the World Ocean Database quality control procedure. One condition we reconsider before rejecting a profile is its vertical resolution. We retain profiles with coarse vertical resolution within the mixed layer itself. But we reject the profile if the vertical resolution is insufficient to resolve the bottom of the mixed layer (if the deepest horizon within the mixed layer is separated from the shallowest horizon below the mixed layer by more than 20% of the mixed layer depth estimate), or if the profile is shallower than the MLD. This latter restriction is important because insufficient vertical resolution leads systematically to under-estimation of MLD.

After estimating MLD, mixed layer temperature, and mixed layer salinity at each profile location we then apply subjective quality control to remove 'bulls eyes' and bin the data into 2^{o}x2^{o}x1mo bins with no attempt to fill in empty bins. The data coverage provided by each instrument is illustrated in **Fig.1a,** expressed as the number of data filled points for each monthly grid (there are approximately 11000 ocean grid points on a 2x2 deg grid). The data coverage is relatively sparse. Even the XBT data never covers more than 20% of the ocean surface in a month.

As indicated in **Fig.1a**, the data coverage provided by each instrument is inhomogeneous in time. Moreover, significant changes in instrumentation have occurred at the beginning of the

1970s due to the introduction of high vertical resolution XBTs. We evaluate possible introduction of instrument bias into the MLD estimates by comparing the December-April MLD calculated from high vertical resolution data (XBT) with MLD calculated from low vertical resolution data (MBT) during 1970-1975 (**Fig. 1b**). The mean MBT-based MLD in the North Atlantic (0N to 70N) is 67m while the XBT-based MLD is 74m. The mean MBT-based MLD in the North Pacific is 67m while the XBT-based MLD is 66m. The comparison shows little evidence of instrument bias in the MLD estimates.

Much of the interesting variability of the mixed layer is linked to a particular phase of the seasonal cycle. Thus, in many of the analyses presented here we examine year-to-year variations of seasonal or bi-season average values. For comparisons to surface winds and SST we rely on the NCEP/NCAR reanalysis (*Kalnay et al., 1996*) and Hadley Center SST analysis (*Rayner et al., 2003)*.

3. Gross Statistics

The climatological monthly maximum and minimum MLDs are shown in **Fig. 2** (lefthand panels show estimates based on temperature, while middle panels show estimates based on density). In the Northern Hemisphere the seasonal maximum depths occur in the subpolar North Atlantic in winter and early spring, with depths exceeding 150m in a region extending well into the western subtropical Atlantic. There the temperature-based estimates of MLD are shallower by around 50m in boreal winter than the density-based estimates because of compensation of temperature and salinity contributions to density (**Figs. 2a, 2b,** also see Fig. 9 in *de Boyer Montegut et al., 2004* for comparisons). Maximum MLDs in the North Pacific are

somewhat shallower than the North Atlantic, falling in the range of 100-200m. Both regions have shallow 10-30m capping mixed layers in boreal summer and fall.

In the tropical Pacific the maximum MLD may exceed 75m in the central basin, decreasing to less than 40m in the east. In the western equatorial Atlantic the temperature criterion indicates the presence of mixed layers deeper than 75m, but the density-based criterion shows that this region of high precipitation and river discharge has a barrier layer at a shallower depth (*Pailler et al., 1999; Foltz et al., 2004*) in contrast to the density compensated layers in the subduction zone in the subtropics. The maximum MLD develops by the end of February-March in the North Pacific and Atlantic (**Figs. 2j, 2k**). The annual phase of the maximum mixed layer changes approaching the equator reflecting the seasonal changes in winds and clouds over the tropics. In the Indian Ocean MLDs in excess of 75m appear in the Arabian Sea during the Southwest Monsoon beginning in June (**Figs. 2a, 2j**).

We compare our analysis to the analysis of *White (1995)* (**Fig. 2**, righthand panels). This alternative analysis has been used extensively to examine the impact of interannually varying mixed layers on winter SST in northern oceans (e.g. *Schneider et al., 1999; Alexander et al., 1999; Timlin et al., 2002; Deser et al., 2003*). The differences in the analysis procedures lead to deeper estimates of MLD in the *White* analysis in the North Pacific as well as the North Atlantic during winter and spring when the upper ocean is weakly stratified. The summer mixed layers, in contrast, are generally shallower in northern latitudes and so the annual range of MLDs is larger and implied entrainment greater in the *White* analysis than in either our temperature-based or density-based analyses. These differences can be attributed to the larger $\Delta T=1C$ criterion (referenced to the surface rather than to 10m depth temperature) adopted in the *White* analysis. In the tropics, mixed layers in the *White* analysis show a similar or smaller annual range, implying

similar rates of entrainment produced by the mixed layer deepening (compare **Figs. 2g** and **2i**). Maximum deepening of the mixed layer and thus maximum entrainment occurs approximately a month later in the *White* analysis.

We next consider the root-mean-square variability in MLD about its climatological monthly average (**Fig. 3**). Here data is segregated by season and is only plotted if available for at least 15 of the 45 years. The available data is mainly confined to the Northern Hemisphere, coastal zones of the Southern Hemisphere, and parts of the west Pacific. The largest variability is confined to the subpolar Atlantic in winter and spring where values in excess of 100m are common. Winter-spring mixed layer variability in the Kuroshio extension region of the western North Pacific (40-75m) is weaker than that in the Gulf Stream and Gulf Stream extension regions of the North Atlantic where it ranges 50-100m. In all of these regions the variability of MLD is 25-50% of the seasonal maximum MLD (compare **Figs. 2** and **3**). Elsewhere the variability is less than 40m. In the tropics variability in the range of 15-30m occurs in all seasons in the Pacific and during the monsoon season (JJA) in the Arabian Sea. Low variability, below 15m, is a feature of the subtropical oceans during summer as well as the eastern tropical Pacific and Atlantic where the mixed layer is shallower. A zonal band of weak variability is particular noticeable along 10N in boreal fall and winter in the Pacific and Atlantic Oceans (**Figs. 3a, 3d**). This low variability band is the result of the shoaling of the thermocline on the northern side of the North Equatorial Counter Current.

The corresponding estimates of MLD variability for the *White (1995)* analysis (**Fig. 3** righthand panels) also have a higher level of MLD variability in the winter Hemisphere. But MLD variability is substantially lower in the highest variability region of the North Atlantic, a difference that probably reflects the higher spatial averaging of the *White* analysis. In the North

Pacific the seasonal timing and geographic location of the maximum variability both differ. The maximum MLD variability according to the *White* analysis is shifted towards the Gulf of Alaska sector of the eastern North Pacific with low variability in the Kuroshio extension region of the western North Pacific. The maximum variability is concentrated in boreal winter and spring (in line with our estimates) but persists into the boreal summer in the central North Pacific. In the *White* analysis the tropics have significantly lower variability throughout the year that in our analysis.

Throughout much of mid latitudes the normalized standard deviation of MLD during the month of maximum deepening exceeds 30% of its depth (**Fig.3e**). In contrast the *White* analysis has significantly lower variability (**Fig. 3j**). MLD variability weakens in the tropics, but is amplified in the equatorial Pacific reflecting the El Nino Southern Oscillation (ENSO) variability (**Fig.3e**). The normalized mixed layer variability in the Atlantic is stronger than in the Pacific. This stronger variability is particularly noticeable in the southern Labrador Sea (prone to the deep convection) and along the western boundary region. Higher MLD variability in the Gulf Stream area as compared to the Kuroshio extension area may be explained by lager spatial gradients of the maximum MLD (see **Fig. 2a**) that result in a stronger contribution of the advective processes that augment variability due to the local forcing.

The frequency dependence of the MLD variability is presented in **Fig. 4** by decomposing the variability into frequencies between $1yr^{-1}$ and $1/5\ yr^{-1}$ (interannual) and frequencies below $1/5\ yr^{-1}$ (decadal). In order to improve the reliability of the statistics we average the results over a winter-spring season (December–April) and a summer-fall season (July-October). During December–April most variability at both interannual and decadal frequencies is confined to higher latitudes. There the variability is at least a factor of two larger in the interannual band than

the decadal band. In contrast to this, during July-October the variability at higher latitudes of the Northern Hemisphere is greatly reduced while it is increased in the Southern Hemisphere during local winter.

In the tropical Pacific the mixed layer variability has a weak seasonal dependence, while in the eastern tropical Indian Ocean and the Arabian Sea the boreal summer variability at interannual frequencies (10-15 m) is higher than that in the boreal winter variability (8-12 m). Boreal summer mixed layer variability is also higher than winter variability in the western tropical Atlantic reflecting the northward shift of the Intertropical Convergence Zone and the accompanying seasonal amplification of the southeasterly trade winds. It should be noted that the partitioning of variance in **Fig. 4** depends on the definition of the decadal and interannual bands. We found that for the 45-yr long time series the standard deviation of the MLD in the decadal band drops by around 25% if the frequency separating the two bands is shifted to $f = 1/8$ yr^{-1}.

Interestingly, part of the decadal variability reflects deepening trends in MLD in the subtropics and mid latitudes (**Fig. 5**). In the North Pacific the most rapid changes occur early in the record from 1960-74 to 1975-1989, consistent with the independent MLD analysis of *Polovina et al.* (1995). *Polovina et al.* have attributed this deepening of the MLD to the climate shift over the north Pacific in the mid-1970s which is reflected in changes in the PDO Index.

Detection of decadal trends is complicated by change in the ocean instrumentation discussed in Section 2. To determine the impact of instrumentation we also present decadal averages using only high vertical resolution instruments (**Fig.5,** XBTs and CTDs). The deepening of the mixed layer in the North Pacific between 1960-1974 and 1975-1989 seen in the 'all data' analysis is also evident in the high resolution analysis (compare **Figs. 5a, 5c** with

Figs.5b, 5d). In contrast, there is only a weak suggestion of the mixed layer deepening in the North Pacific between 1975-1989 and 1990-2004. In the tropical Pacific and Atlantic Oceans there is little evidence of decadal trends in MLD.

In the Atlantic the 'all data' analysis suggests a steady mixed layer deepening along and south of the Gulf Stream front. The high vertical resolution analysis is patchier due to lower data coverage. North of 45N, both the 'all data' and high resolution analyses show a transition from shallow mixed layers during 1960-1974 (**Figs. 5a, 5b**) to deeper mixed layers during 1990-2004 (**Figs. 5e, 5f**). This long term deepening reflects the impact of the strengthening surface forcing and associated strengthening of westerly winds and increasing net surface heat loss.

In the north Atlantic subpolar gyre the deepening of the mixed layer has occurred while the water column has cooled and freshened (*Dickson et al*., 2002). Because of its relationship to surface forcing as well as to entrainment cooling of the mixed layer, these variables may not be independent. We examine the potential connection between MLD and SST by computing the time regression of their anomalies with respect to the climatological seasonal cycle (**Fig. 6**). During all seasons this correlation analysis reveals the importance of surface forcing in northern latitudes where deeper than normal MLDs are associated with cooler than normal mixed layer temperatures. The regression coefficient is larger in winter reflecting the impact of entrainment deepening. In contrast, in the eastern half of the tropical Pacific we have the relationship frequently assumed in models of ENSO that deeper than normal MLDs are associated with warmer than normal mixed layer temperatures. A similar relationship is evident in the tropical Indian and Atlantic basins during June-August and in the western tropical Pacific during December-February, and along the western boundaries. This positively correlated relationship suggests that the anomalous heat budget of the mixed layer is dominated either by heat exchange

across the bottom of the mixed layer (in the upwelling areas) or by horizontal heat advection (in the frontal areas along the western boundaries).

4. Variability in the Northern Oceans during Winter-Spring

Despite similar latitudes, SSTs, and presence of winter storms, mixed layers in the North Pacific and North Atlantic differ in several fundamental ways. The near-surface waters of the North Pacific are more stratified, while the higher salinity waters of the North Atlantic mixed layers are affected by episodic freshening events (*Belkin, 2004*). In this section we explore the relationships between MLD, SST, and winds in these two regions by application of Empirical Orthogonal Eigenfunction (EOF) analysis.

The domain for the first EOF analysis spans the North Pacific and is similar to that chosen by *Bond et al. (2003)* for their EOF analysis of November-March SST. Our analysis is based on the five month December-April averages when the mixed layer depth is at its seasonal maximum. The primary EOF of MLD explains 9.5% of the record variance with maximum variance in the central basin between 30^{o}N-50^{o}N and positive values almost everywhere, indicating an in-phase response across the basin (**Fig. 7a**). The projection of the component time series on surface winds shows that the region of maximum MLD change is almost precisely associated with the corresponding region of maximum wind speed change (**Fig. 7c**). The second EOF of MLD (not shown), explains 6.5% of the record variance. This second EOF has a dipole pattern with a peak in the subtropical western basin along the climatological position of the Kuroshio front and peaks of opposite phase in the northern central and eastern regions.

The principal component time series associated with this primary EOF (**Fig. 7b**) shows a long-term deepening trend including a rapid 10m deepening in the mid-1970s, consistent with

the 15-year averages shown in **Fig. 5**. Superimposed on this long-term trend, the time series in **Fig. 7b** also reveals strong winter-to-winter fluctuations with an alternating succession of shallow and deep wintertime mixed layers in the mid-1970s through the 1980s.

Modeling studies (e.g., *Alexander et al., 2000; Xie et al., 2000)* have connected the year-to-year fluctuations in MLD to changes in local competing processes of turbulent exchange and buoyancy flux, which together regulate entrainment rate. We explore this connection by comparing the first principal component time series with the December-April PDO index reflecting low frequency changes of SST in the North Pacific. The PDO Index and the first principal component time series are positively correlated (r = 0.75 with modest smoothing) with similar year-to-year variability as well as long-term trends. Interestingly, *Cummins et al.* (2005) have demonstrated that sea level in this region also varies in phase with the PDO index, suggesting the changes of temperature and salinity penetrate throughout the upper ocean water column.

Finally, we examine the connection between winter-spring MLD and SST in the region of strong MLD-wind coherence (180^{o}-150^{o}W, 35^{o}-45^{o}N box is shown in **Fig. 7a**). In this region SST has a negative phase relationship with MLD where a 10m deepening of the MLD is associated with a 0.5^{o}C drop in SST (correlation is r=-0.48, **Fig. 8a**). Thus, anomalously deep MLD is associated with anomalously cool SST. The physics of this relationship is not entirely clear. The regression patterns in **Fig.7c** also show a positive relationship between mixed layer deepening and surface heat loss with both patterns centered at around 40N consistent with previous studies (*Alexander et al.,* 2002; *Qu,* 2003). The strongest mixed layer response is found at around 160W just where the wind speed response peeks (compare **Figs. 7a, 7c**), while the surface heat flux pattern peeks to the east at 160E. Thus, likely both entrainment and surface heat

fluxes are important in regulating year-to-year SST variations at this location in the central North Pacific.

We next turn to the North Atlantic where depth variability is a factor of two larger than the North Pacific (**Fig. 3**) and where variability in excess of 75m extends from the eastern subpolar region to the western subtropics. This zone is also where winter-spring MLDs extend deeper than 100m. Here we address the nature of this high variability and its connection to changes in surface meteorology.

The primary EOF in a domain extending from the equator to 70^{o}N explains 13% of the record variance and is mainly confined to the high MLD variability zone extending from the eastern subpolar region to the western subtropics (**Fig. 9**). The western half of this zone lies just to the east of the Gulf Stream front. The relative position of features suggests that the variability of MLD may be associated with shifts in the Gulf Stream frontal position rather than with variability of local winds. Indeed, the projection of the surface winds onto the primary principal component time series shows that deepening of the MLD is correlated with increasing westerly winds at subpolar latitudes and increasing northeast trade winds in the tropics. This wind pattern resembles the wind pattern associated with strengthening of the Azores high in sea level pressure.

The corresponding principal component time series (**Fig. 9b**) shows that the mixed layer has deepened in this zone since the 1960s by more than 40m. A similar long term change is evident in the NAO Index, reflecting changes in the position of the storm tracks. Relationships between changes in the NAO Index and changes in the Gulf Stream frontal position have been explored by *Taylor and Stephens (1998*) who showed a delayed (by a few years)

northward/southward shift of the front in response to amplification/attenuation of the NAO Index.

As in the case of the North Pacific, the time series shows considerable year-to-year variability. The relationship of MLD, wind, and SST variability also is not nearly as close in the North Atlantic as in the North Pacific. Time series of these variables are displayed in **Fig. 8b** for a rectangular box spanning the central basin (60^o-30^oW, 35^o-45^oN, see **Fig.9a)**. Within this box MLD and SST both exhibit a positive trend since the mid-1960s, but correlations between those variables at year-to-year timescales are quite weak.

5. Tropics

While mixed layer variability is weaker in the tropics than in the northern oceans (**Fig. 3)** some coherent features are evident. The predominant pattern of MLD variability in the tropical Pacific is coherent with the Southern Oscillation Index (SOI) and thus is associated with ENSO (**Fig. 10**). Here we restrict our analysis to the peak months of the mature phase of ENSO (November-March). A 10-20 decrease in the SOI, corresponding to the appearance of El Niño, is correlated with a concurrent deepening of the tropical MLD in the eastern Pacific by 5-15m and a shallowing in the western Pacific and eastern Indian Ocean by 10-20m. In the eastern equatorial Pacific *Wang and McPhaden (2000)* found that the strong El Niños of 1982-3 and 1997 were associated with mixed layer deepenings of 30m or more at 0^oN, 110^oW (*Cronin and Kessler, 2002* also examine the 1997 event). The weakening of upwelling associated with these deepening mixed layers was found to be an important modification of the mixed layer heat budget at this location. In **Fig. 11a** we determine a similar relationship for oceanic variables averaged over the NINO3 region (150^oW-90^oW, 5^oS-5^oN). Averaged annually (to improve the

statistics), the vertical excursions of MLD reduce to a more modest 10m. However, there remains a similarly close relationship between increasing SST and a deepening mixed layer (with a ratio of 0.1^{o}C/m) and NINO3 MLD leading NINO3 SST by a few months (**Fig.11c)**, as well as between increasing NINO3 SST and decreasing zonal wind speed in the west (**Figs. 11a, 11b**). Winds in the west lead SST in the east by a few months (**Fig.11c**). In the western equatorial Pacific we find, similar to *Wang and Mcphaden*, that substantial variations in MLD are evident (**Fig. 11b**), which lag variations in local winds by several months (**Fig.11c**). These MLD variations are not closely related to variations in local SST (**Fig. 11b**) suggesting a minor impact of entrainment on the mixed layer heat balance in the west.

The extension of the ENSO response into the mid latitude North Pacific has been examined by *Alexander et al.* (2002) (see their Fig.9). Consistent with their results, we find anomalous mixed layer deepening in the central North Pacific in the latitude range 30N to 45N during El Ninos. This anomalous deepening of the mixed layer occurs concurrent with anomalous cooling (**Fig.8a**, see also Fig.5 of *Alexander et al*. 2002) suggesting the importance of anomalous surface heat loss. In contrast, in the tropics the mixed layer warms as it deepens (**Figs. 6** and **10a**) in response to heat exchanges across the base of the mixed layer.

As discussed in the Introduction, it has been suggested that anomaly mixed layer patterns can persist from one winter to the next in conjunction with the re-emergence of SST patterns (*Alexander et al*., 2001). We explore the persistence of MLD patterns between successive winters by examining the regression of the SOI index on the next winter (Y+1) anomaly MLD. The midlatitude mixed layer during the next winter (**Fig.10b**) shows the persistence of a deepening pattern around 35N with shallowing to the north and south. Interestingly, net surface

flux response does not show similar persistence. In the tropics, in contrast, the mixed layer is anomalously shallow during the following winter.

The extension of the ENSO response into the eastern tropical Indian Ocean (**Fig. 10a**) is also evident in our examination of the primary EOF of MLD during December-February (**Fig. 12a**). The spatial pattern of the mixed layer response associated with this EOF, which explains 9.5% of the record variance, has a maximum in the eastern tropics. The pattern extends further south along the Sumatra coast, with a minimum south of the equator in the central basin. The corresponding principal component time series shows that this pattern is closely related to the SOI so that MLD along the equator in the east is shallow during El Niños. Interannual variations of the mixed layer during boreal winter seem to be connected to the local wind response to ENSO. MLD variations are confined primarily to the eastern and central basin and reflect changes of the equatorial and coastal upwelling in the east and the pattern of Ekman pumping produced by the cyclonic winds in the south central basin (**Fig. 12a**) (see also *Murtugudde et al.*, 1999; *Potemra and Lukas*, 1999; and *Grodsky et al*., 2001). In contrast to the conditions in December-February, the primary EOF during the peak season of the Southwest Monsoon in boreal summer reveals MLD variability confined to the western basin (**Fig. 12b**). During this season variations in MLD are associated with changes in the strength of the monsoonal winds, as also suggested in recent studies by *Prasad (2004)* and *Babu et al. (2004).*

6. Summary and Discussion

In this work we apply the methodology of *de Boyer Montegut et al*. (2004) to construct a monthly analysis of global mixed layer depth during the 45-year period 1960-2004 based on profiles from the new WOD05 data set. The data set is limited in temporal and geographic

coverage, and thus averaging is required to identify year-to-year variability. The problem of limited data is magnified since much of the MLD variability is linked to the seasonal cycle.

Despite the data limitations (which restrict our analysis to the Northern Hemisphere and tropics) we explore the historical record for variability that is coherent with variability appearing in winds and SST. We begin by comparing the new analysis with the widely used analysis of *White* (1995). Our analysis differs in having shallower winter mixed layers, especially in the North Pacific. Our analysis also has shallower summer mixed layers, while the climatological peak in entrainment rate occurs a month earlier than in the *White* analysis. The distribution of MLD variability about its climatological monthly cycle also differs between the two data sets, with shifts in amplitude, structure, and seasonality.

We next consider the spatial and temporal structure of MLD variability in each of the three ocean basins and their relationship to winds and SST. In the Pacific the highest variability occurs in the subtropics and midlatitudes in the western half of the basin during boreal winter-spring. During this season 2/3 of the variability occurs at frequencies less than 1/5 yr^{-1}. An EOF decomposition of winter-spring MLD in the North Pacific reveals that some of this interannual variability is associated with a stationary pattern with a maximum in the domain 180E-150^{o}W, 35^{o}-45^{o}N. The time variability of this primary EOF closely resembles the winter-spring PDO Index, reflecting a correspondence between increases in the MLD and increases in local wind speed. SST varies out of phase with wind speed, and thus increases in winter-spring SST are associated with shallower than normal MLD.

In boreal summer MLD variability in both the Pacific and Atlantic is reduced and tropical variability becomes more distinct. There the largest coherent signal is associated with ENSO. During an El Niño the annually averaged MLD in the eastern Pacific is deeper by 10m (and thus

there is a positive correlation between SST and MLD), while MLD in the western Pacific and the eastern Indian Oceans is shallow by 10-15m.

In the Atlantic the highest variability also occurs in the subtropics and midlatitudes during boreal winter-spring, and with much of the variability at interannual frequencies. An EOF analysis shows that the maximum coherent MLD variability occurs in a zone extending along the eastern edge of the Gulf Stream in the western subtropics northeastward toward the eastern subpolar region. In contrast to the North Pacific, the MLD variability in this region is not closely related to variations in local wind speed, and does not result in coherent variations in winter SST.

A notable feature of both the central North Pacific and North Atlantic is the presence of trends that have caused the mixed layer to deepen by 10-40m over the past 45 years. In the North Pacific this deepening trend is matched by a corresponding increasing trend in the PDO Index. The presence of this trend in PDO, indeed, explains much of the decadal variability in the North Pacific MLD. Strikingly, much of the change in MLD occurred early in the record, prior to the 1980s. In the North Atlantic this deepening trend is likewise reflected in a positive trend in the NAO Index.

The salinity data coverage is still a limiting factor to address the interannual variations of the barrier and density compensated layers.

Acknowledgements

We gratefully acknowledge the Ocean Climate Laboratory of the National Oceanographic Data Center/NOAA, under the direction of Sydney Levitus for providing the database upon which this work is based. The JEDA Center, under the leadership of Warren White, has kindly made its MLD estimates available to the community. We found reviewers

comments to be helpful and stimulating. Support for this research has been provided by the National Science Foundation (OCE0351319) and the NASA Physical Oceanography Programs.

7. Appendix

We use both temperature-salinity and temperature only profiles to compute mixed layer depth. Here we consider three situations in which the estimates may differ. The examples are from North Atlantic during boreal winter when the temperature stratification is weak and the impact of salinity is stronger. In **Fig. Aa** temperature drops below the density-based mixed layer producing a 50m width barrier layer. In contrast, in **Fig. Ab** temperature increases below the salinity-based mixed layer producing a density compensated layer. To provide an MLD estimate consistent with its description as a layer of uniform properties in this situation we modify the definition of the mixed layer chosen by *de Boyer Montegut et al*. (2004). We define the base of the mixed layer to be the depth at which temperature either drops or rises by 0.2^{o}C. Finally in **Fig. Ac** we see a second example of a density-compensated mixed layer in which both temperature and salinity decrease below the mixed layer. Our modified definition also produces consistent estimates in this situation.

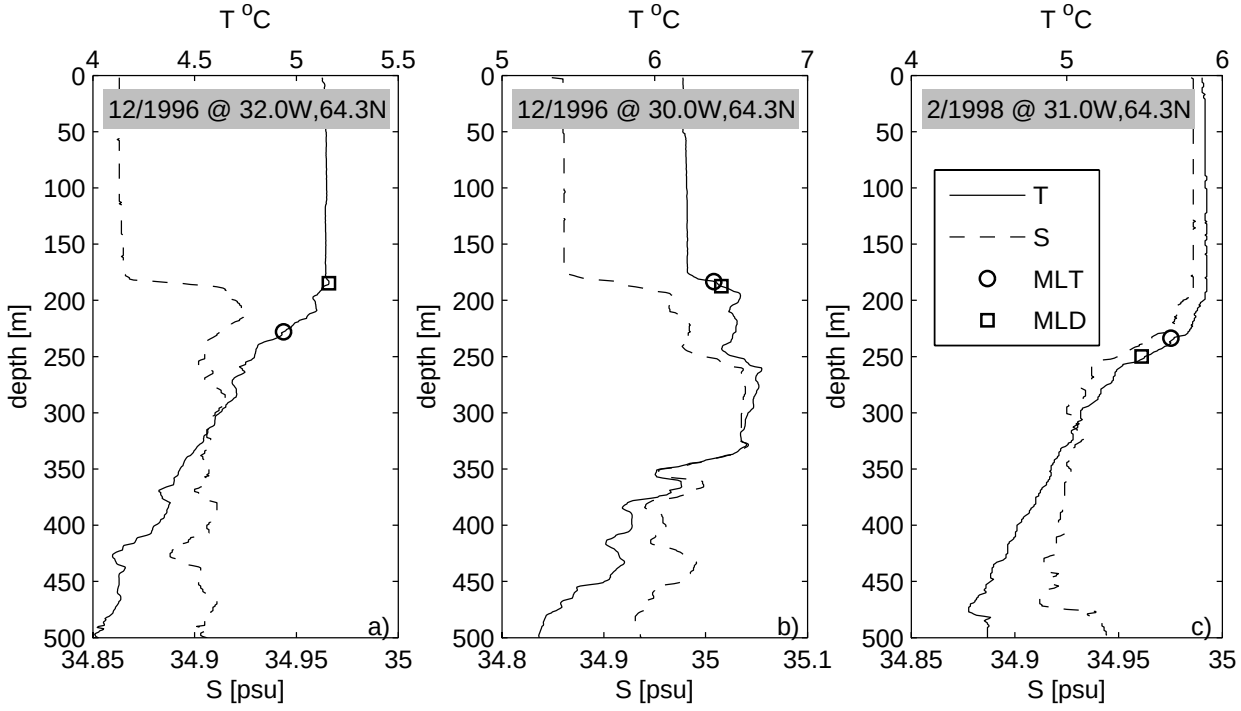

Figure A. Sample *T* and *S* vertical profiles taken in the north Atlantic during winter. *MLT* and *MLD* are the mixed layer depth estimates based on the $|\Delta T|$=0.2 °C and $\Delta\sigma = \partial\sigma/\partial T \cdot 0.2$°C, respectively.

References

Alexander, M.A., C. Deser, and M.S. Timlin, 1999: The reemergence of SST anomalies in the North Pacific Ocean, *J. Clim.*, **12**, 2419-2433.

Alexander, M.A., J.D. Scott, and C. Deser, 2000: Processes that influence sea surface temperature and ocean mixed layer depth variability in a coupled model, *J. Geophys. Res*, **105**, 16823-16842.

Alexander, M.A., M.S. Timlin, and J.D. Scott, 2001: Winter-to-winter recurrence of sea surface temperature, salinity and mixed layer depth anomalies, *Progr. Oceanogr.*, **49** , 41–61.

Alexander, M.A., E. Blade, M. Newman, J.R. Lazante, N.-C. Lau, and J.D. Scott, 2002: The Atmospheric Bridge: The Influence of ENSO Teleconnections on Air–Sea Interaction over the Global Oceans, *J. Clim.,* **15**, 2205-2231.

Babu, K.N., R. Sharma, N. Agarwal, V.K. Agarwal, and R. A. Weller, 2004: Study of the mixed layer depth variations within the north Indian Ocean using a 1-D model, *J. Geophys. Res*, **109**, C08016, doi:10.1029/2003JC002024.

Barnston A.G., and R.E. Livezey, 1987: Classification, Seasonality and Persistence of Low-Frequency Atmospheric Circulation Patterns, *Mont. Wea. Rev.*, **115**, 1083-1126.

Bates, N.R., 2001: Interannual variability of oceanic CO2 and biogeochemical properties in the Western North Atlantic subtropical gyre, *Deep-Sea Res.* II, **48**, 1507-1528.

Belkin, I.M., 2004: Propagation of the ‘‘Great Salinity Anomaly’’ of the 1990s around the northern North Atlantic, *Geophys. Res. Lett.*, **31**, L08306, doi:10.1029/2003GL019334.

Bond, N.A. J.E. Overland, M. Spillane, and P. Stabeno, 2003: Recent shifts in the state of the North Pacific, *Geophys. Res. Lett.*, **30**, doi:10.1029/2003GL018597.

Boyer, T.P., J.I. Antonov, H.E. Garcia, D.R. Johnson, R.A. Locarnini, A.V. Mishonov, M.T. Pitcher, O.K. Baranova, and I.V. Smolyar, 2006: *World Ocean Database 2005.* S. Levitus, Ed., NOAA Atlas NESDIS 60, U.S. Government Printing Office, Washington, D.C., 190 pp., DVDs.

Boyer, T. P., S. Levitus, J. I. Antonov, R. A. Locarnini, and H. E. Garcia, 2005: Linear trends in salinity for the World Ocean, 1955–1998, *Geophys. Res. Lett*., **32**, L01604, doi:10.1029/2004GL021791.

Chai, F., M. Jiang, R. T. Barber, R. C. Dugdale, and Y. Chao, 2003: Interdecadal Variation of the Transition Zone Chlorophyll Front: A Physical-Biological Model Simulation between 1960 and 1990, *J. Oceanog.*, **59**, 461 – 475.

Chavez, F.P., J. Ryan, S.E. Lluch-Cota, and M. Niquen C, 2003: From anchovies to sardines and back: Multidecadal change in the Pacific Ocean, *Science*, **299**, 217-221.

Cronin, M.F., and W.S. Kessler, 2002: Seasonal and interannual modulation of mixed layer variability at 0N, 110W, *Deep-Sea Research I*, **49**, 1–17.

Cummins, P. F., G. S. E. Lagerloef, and G. Mitchum, 2005: A regional index of northeast Pacific variability based on satellite altimeter data, *Geophys. Res. Lett.*, **32**, L17607, doi:10.1029/2005GL023642.

Curry, R., R. Dickson, and I. Yashayaev, 2003: Ocean evidence of a change in the fresh water balance of the Atlantic over the past four decades, *Nature*, **426**, 826-829.

de Boyer Montegut, C., G. Madec, A. S. Fischer, A. Lazar, and D. Iudicone, 2004: MLD over the global ocean: An examination of profile data and a profile-based climatology, *J. Geophys. Res.*, **109**, C12003, doi:10.1029/2004JC002378.

Deser, C., M.A. Alexander, and M.S. Timlin, 2003: Understanding the Persistence of Sea Surface Temperature Anomalies in Midlatitudes, *J. Clim.*, **16**, 57-72.

Dickson, R.R., T.J. Osborn, J.W. Hurrell, J. Meincke, J. Blindheim, B. Adlandsvik, T. Vinje, G. Alekseev, and W. Maslowski, 2000: The Arctic Ocean response to the North Atlantic Oscillation, *J. Clim.*, **13**, 2671-2696.

Dickson, B., I. Yashayaev, J. Meincke, B. Turrell, S. Dye, and J. Holfort, 2002: Rapid freshening of the deep North Atlantic Ocean over the past four decades, *Nature*, **416,** 832-837.

Freeland, H., K. Denman, C. S. Wong, F. Whitney and R. Jacques, 1997: Evidence of change in the winter mixed layer in the Northeast Pacific Ocean, *Deep Sea Res. I*, **44**, 2117-2129.

Flatau, M.K., L. Talley, and P.P. Niiler, 2003: The North Atlantic Oscillation, surface current velocities, and SST changes in the subpolar North Atlantic, *J. Clim.*, **16**, 2355-2369.

Foltz, G., S.A. Grodsky, J.A. Carton, and M. J. McPhaden, 2004: Seasonal salt budget of the northwestern tropical Atlantic Ocean along 38W, *J. Geophys. Res.*, **109**, C03052, doi:10.1029/2003JC002111.

Grodsky, S.A., J.A. Carton, and R. Murtugudde, 2001: Anomalous surface currents in the tropical Indian Ocean, *Geoph. Res. Lett*., **28**, 4207-4210.

Hurrell, J.W., 1995: Decadal trends in the North-Atlantic Oscillation - regional temperatures and precipitation, *Science*, **269**, 676-679.

Kalnay, E., and Coauthors, 1996: The NCEP/NCAR 40-year reanalysis project, *Bull. Amer. Meteorol. Soc.*, **77**, 437-471.

Kara, A. B., P. A. Rochford, and H. E. Hurlburt, 2002: Naval Research Laboratory MLD (NMLD) Climatologies, Rep. NRL/FR/ 7330–02-9995, 26 pp., Naval Res. Lab., Washington, D. C.

Levitus, S., J. Antonov, and T. Boyer, 2005: Warming of the world ocean, 1955–2003, *Geophys. Res. Lett.,* **32**, L02604, doi:10.1029/2004GL021592.

Lorbacher, K., D. Dommenget, P. P. Niiler, and A. Köhl, 2006: Ocean MLD: A subsurface proxy of ocean atmosphere variability, *J. Geophys. Res.*, **111**, C07010, doi:10.1029/2003JC002157.

Mantua, N.J., S.R. Hare, Y. Zhang, J.M. Wallace, and R.C. Francis, 1997: A Pacific interdecadal climate oscillation with impacts on salmon production, *Bull. Amer. Meteor. Soc.,* **78**, 1069-1079.

Michaels, A.F. and A.H. Knap, 1996: Overview of the U.S. JGOFS Bermuda Atlantic Time-series Study and the Hydrostation S Program, *Deep-Sea Res.*, **43**, 157-198.

Monterey, G., and S. Levitus, 1997: Seasonal Variability of MLD for the World Ocean, *NOAA Atlas NESDIS 14*, 100 pp., Natl. Oceanic and Atmos. Admin., Silver Spring, MD.

Murtugudde, R., J. P. McCreary Jr., and A. J. Basalacchi, 1999: Oceanic processes associated with anomalous events in the Indian Ocean with relevance to 1997-1998, *J. Geophys. Res*., **105,** 3295-3306.

Nilsen, J. E. Ø., and E. Falck, 2006: Variations of mixed layer properties in the Norwegian Sea for the period 1948–1999, *Prog. Oceanogr., 70,* 58–90.

Pailler, K., B. Bourles, and Y. Gouriou, 1999: The barrier layer in the western tropical Atlantic Ocean, *Geophys. Res. Lett*., **26**, 2069–2072.

Prasad, T. G., 2004: A comparison of mixed-layer dynamics between the Arabian Sea and Bay of Bengal: One-dimensional model results, *J. Geophys. Res.*, **109**, C03035, doi:10.1029/2003JC002000.

Polovina, J.J., G.T. Mitchum, and G.T. Evans, 1995: Decadal and basin-scale variation in MLD and the impact on biological production in the central and North Pacific, 1960-88, *Deep-Sea Res.,* **42***,* 1701-1716.

Potemra, J. T., and R. Lukas, 1999: Seasonal to interannual modes of sea level variability in the western Pacific and eastern Indian Oceans, *Geoph. Res. Let.*, **26**, 365-368.

Qu, T., 2003: Mixed layer heat balance in the western North Pacific, *J. Geophys. Res*., **108**, 3242, doi:10.1029/2002JC001536.

Rayner, N. A., D. E. Parker, E. B. Horton, C. K. Folland, L. V. Alexander, D. P. Rowell, E. C. Kent, and A. Kaplan, 2003: Global analyses of sea surface temperature, sea ice, and night marine air temperature since the late nineteenth century, *J. Geophys. Res.*, **108**, 4407, doi:10.1029/2002JD002670.

Schneider, N., A.J. Miller, M.A. Alexander, and C. Deser, 1999: Subduction of decadal North Pacific temperature anomalies: Observations and dynamics, *J. Phys. Oceanogr.*, **29**, 1056-1070.

Taylor, A.H., and J.A. Stephens, 1998: The North Atlantic Oscillation and the latitude of the Gulf Stream, *Tellus – A,* **50**, 134-142.

Timlin, M.S., M.A. Alexander, and C. Deser, 2002: On the Reemergence of North Atlantic SST Anomalies, *J. Clim*., **15**, 2702-2712.

Wang, W., and M.J. McPhaden, 2000: The Surface-Layer Heat Balance in the Equatorial Pacific Ocean, Part II: Interannual Variability, *J. Phys. Oceanogr.*, **30**, 2989-3008.

White, W.B., 1995: Design of a global observing system for gyre-scale upper ocean temperature variability, *Prog. Oceanogr.,* **36,** 169-217.

Xie, S.-P., T. Kunitani, A. Kubokawa, M. Nonaka, and S. Hosoda, 2000: Interdecadal Thermocline Variability in the North Pacific for 1958–97: A GCM Simulation, *J. Phys. Oceanogr.*, **30**, 2798-2813.

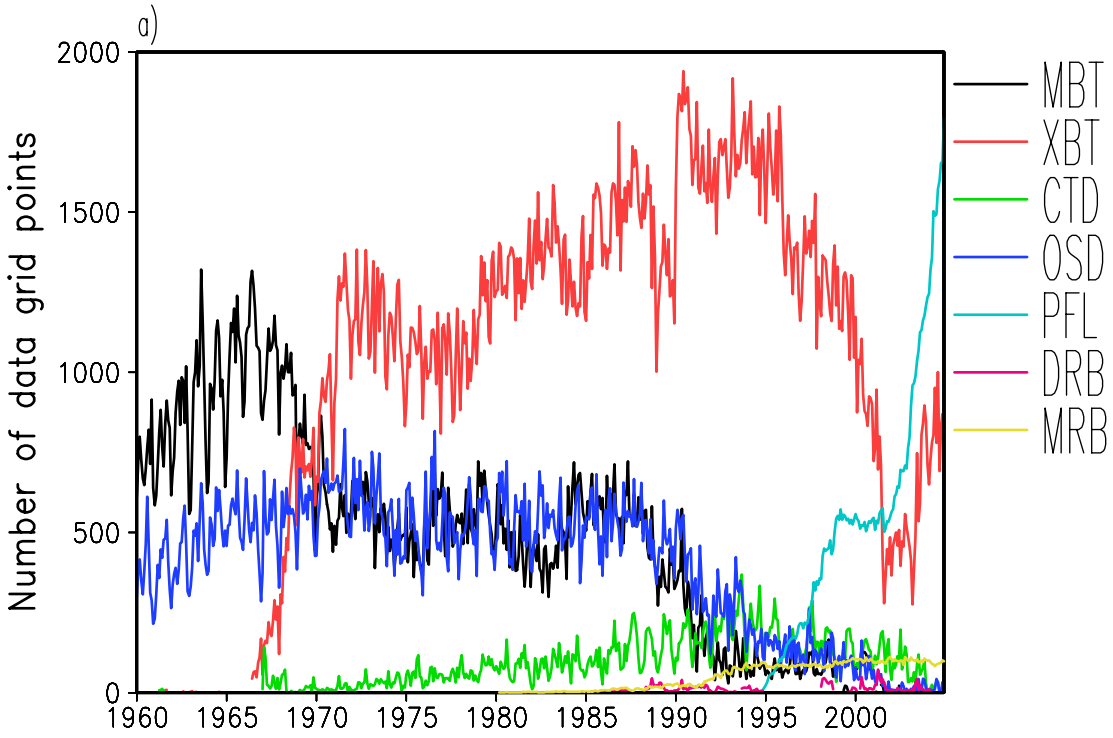

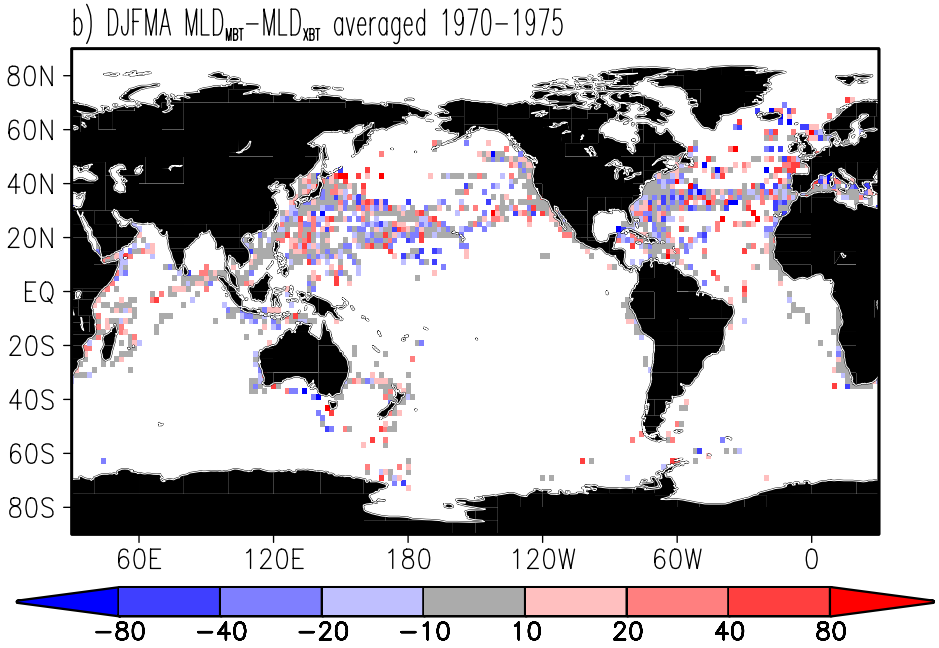

Figure 1. (a) Number of grid points on a 2x2 deg grid filled with data. Data are stratified by instruments. Instrument abbreviations are the same as those adopted in the NODC World Ocean Atlas. Full ocean surface coverage corresponds to approximately 11,000 points. (b) December-April MLD difference (in meters) between MBT-based and XBT-based estimates where both observations are available for the same month.

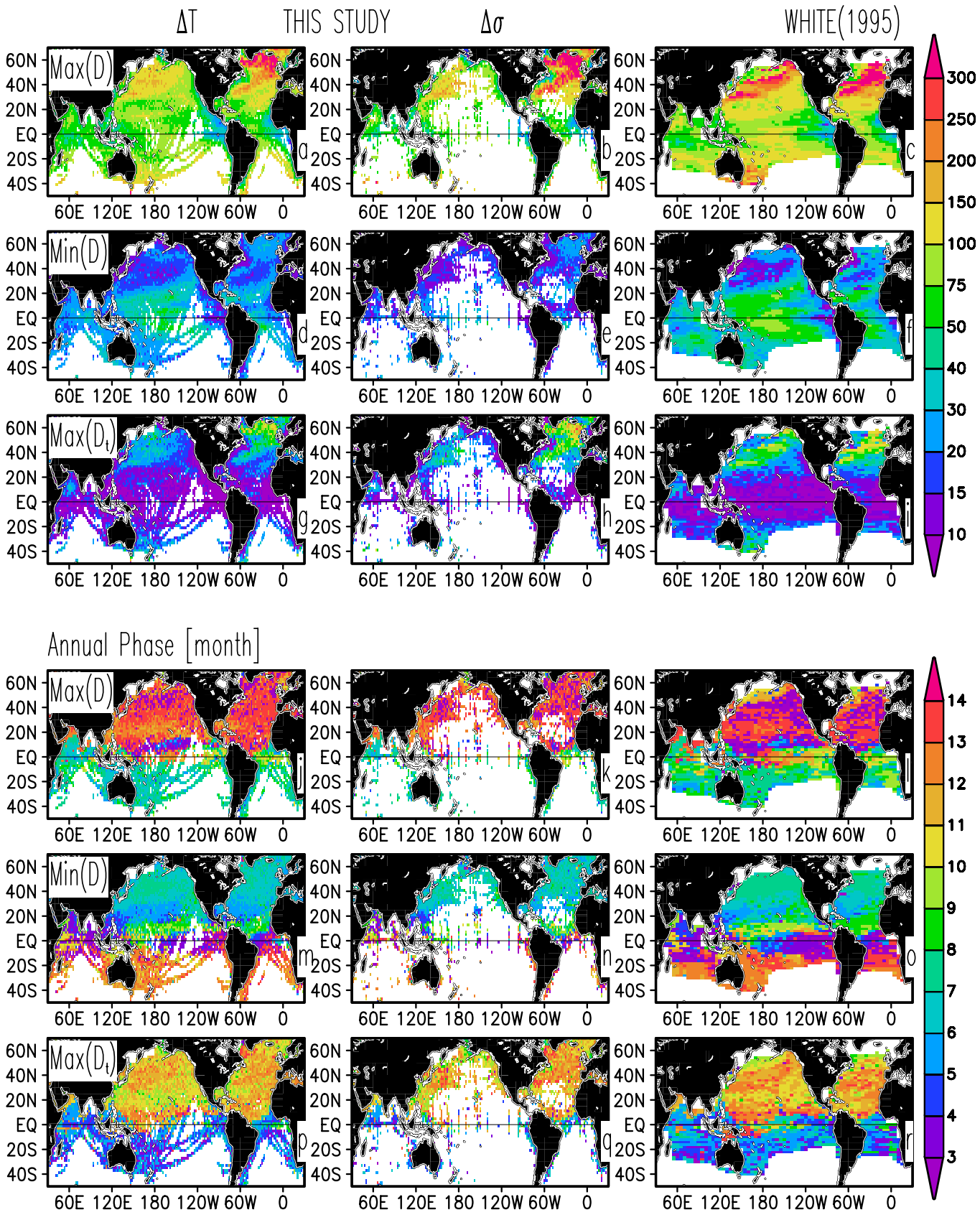
ΔT
THIS STUDY
Δσ
WHITE(1995)
Max(D)
Min(D)
Max(D_t)
a
b
c
d
e
f
g
h
i
60N
40N
20N
EQ
20S
40S
60E 120E 180 120W 60W 0
300
250
200
150
100
75
50
40
30
20
15
10
Annual Phase [month]
j
k
l
m
n
o
p
q
r
14
13
12
11
10
9
8
7
6
5
4
3

Fig. 2 Monthly climatology of the MLD extremes computed over the 1960-2004 period. Left and middle columns show extremes based on the temperature-based definition ($|\Delta T|$=0.2 ^{o}C) and the variable density-based definition. Righthand column shows extremes based on the *White (1995)* analysis averaged over a similar period (1960-2003). Maximum MLD (a,b,c), minimum MLD (d,e,f), maximum entrainment rate (g,h,i), and the month (annual phase) of maximum MLD (j,k,l), minimum MLD (m,n,o), and maximum entrainment rate (p,q,r). Multiply entrainment rate in (g) by $C_p \rho * \Delta T$ = -0.3 to convert to entrainment heat flux in Wm^{-2}.

Estimates are plotted only if observations are available for at least 15 years. Units are meter, meter/month, and month. Month color scale begins in March in order to align with seasonal changes.

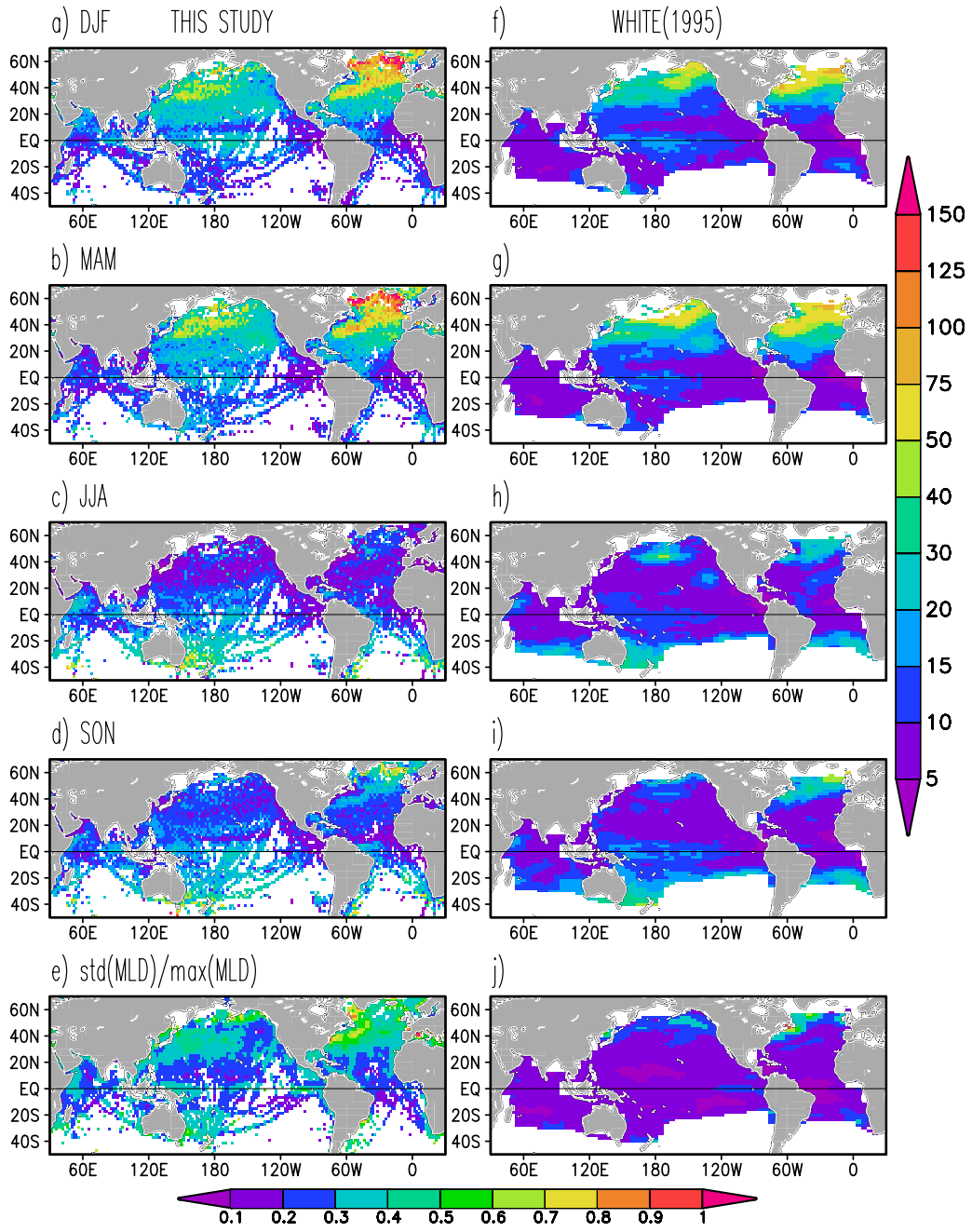

Fig. 3 Standard deviation of mixed layer depth from its climatological seasonal average computed over the full 45-year period. Lefthand panels show results for this study. Estimates are plotted only if observations are available for at least 15 years. Righthand panels show results for the *White (1995)* analysis over 1960-2003. Units are meters. Color scaling is shown with righthand palette. Two bottom panels show the normalized standard deviation of MLD during the month of maximum deepening.

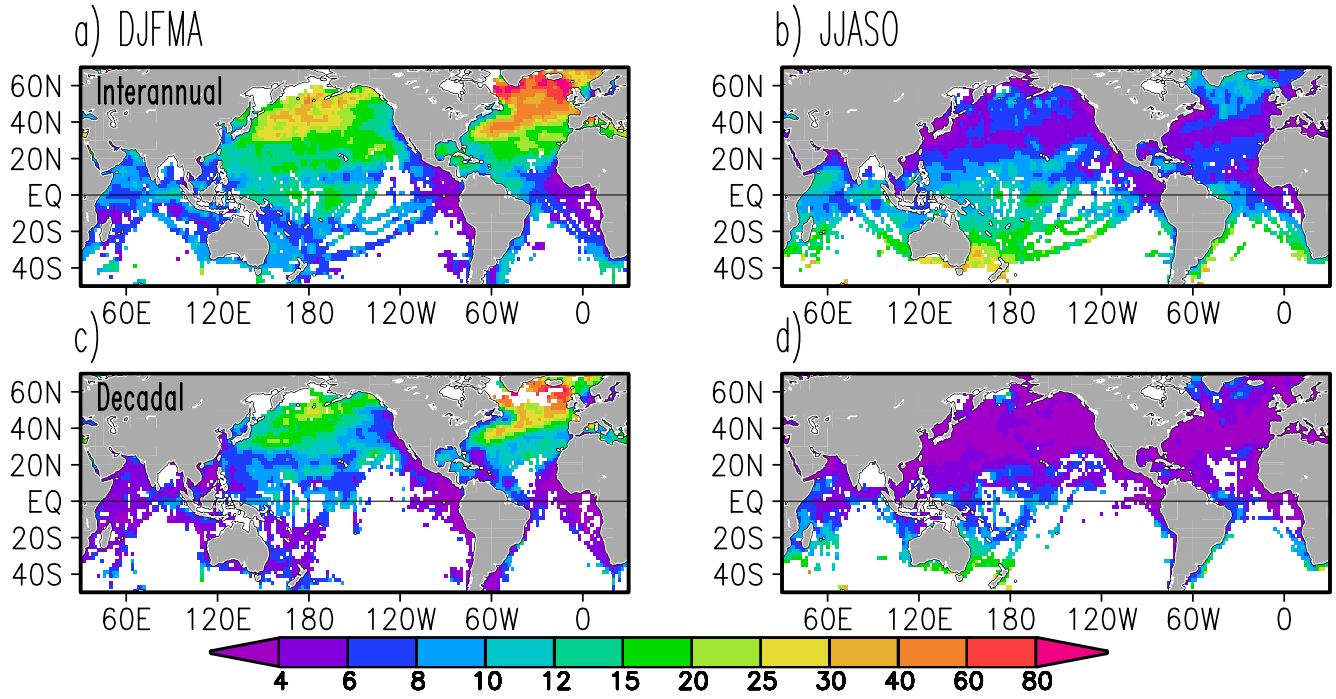

Figure 4 Root-mean-square MLD variability separated into interannual ($1/5yr^{-1}<f<1yr^{-1}$) and decadal frequency bands ($f<1/5yr^{-1}$) and into bi-seasons (left) December-April and (right) June-October. Interannual values are masked out if a grid box has less than 10% data coverage, while decadal values are masked out if the more poorly sampled first half of the record has less than 10% data coverage. Units are meters.

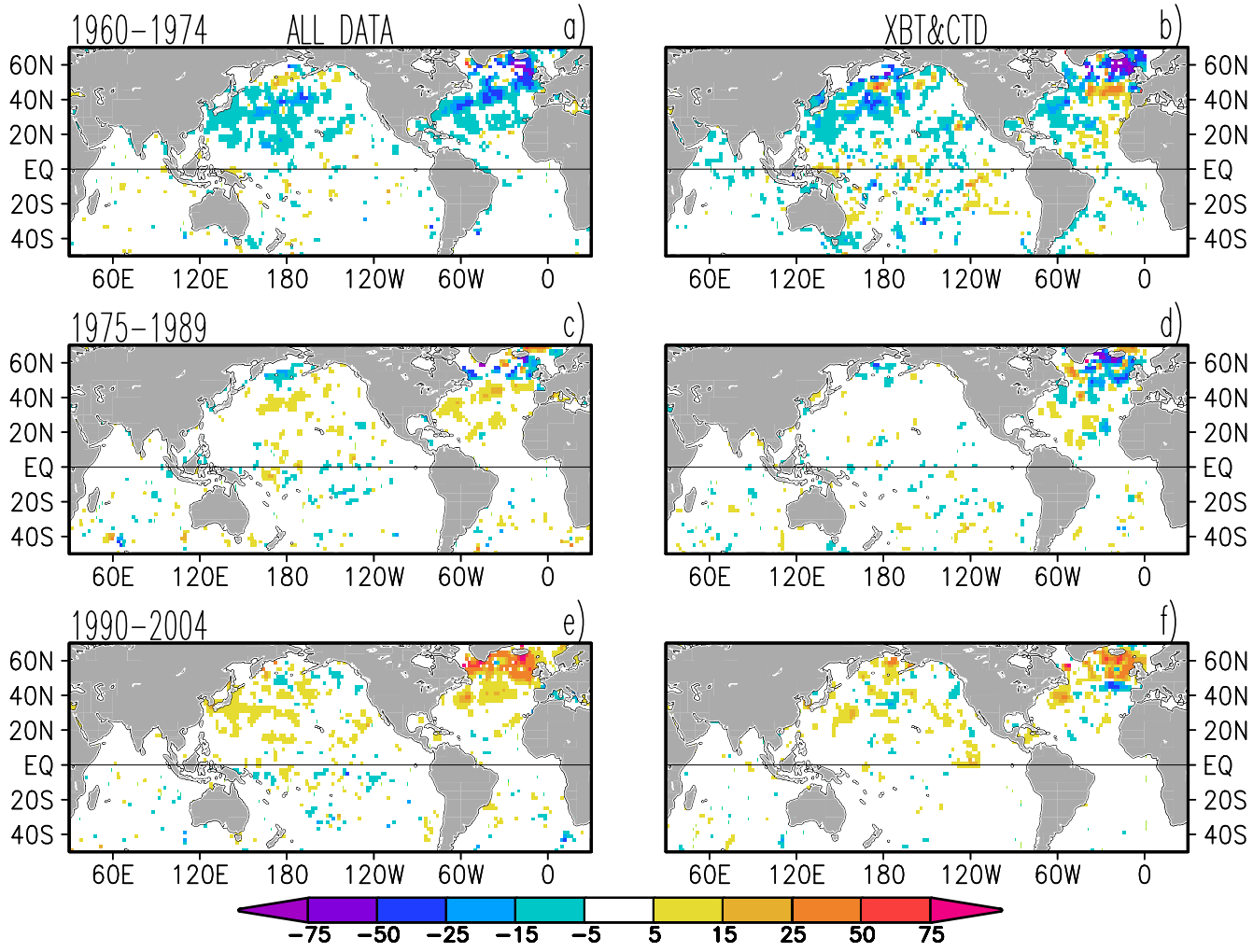

Figure 5 Winter-spring (December-April) MLD anomalies averaged into 15-year intervals (left) based on the whole dataset, and (right) based on the XBT and CTD data only. In the left column grid points with fewer than 15 monthly samples in any 15-year interval are masked out. A deepening trend is evident in the North Pacific and North Atlantic.

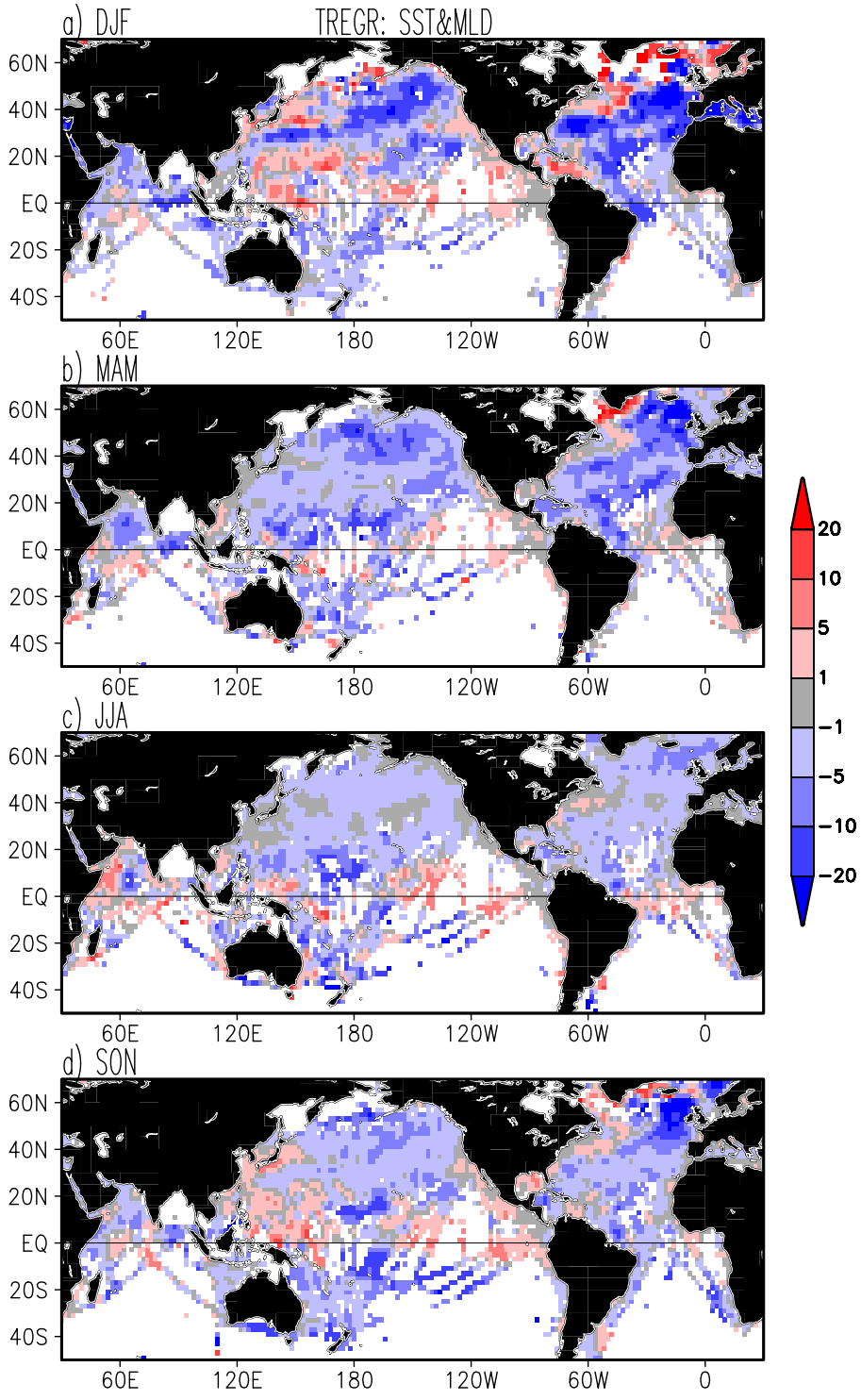

Figure 6 Time regression of mixed layer depth and temperature anomalies from their climatological monthly values averaged by season. Data is shown at grid points where there is at least 15 years of data. Units are m/degC. Temperature is taken from profiles used to calculate MLD.

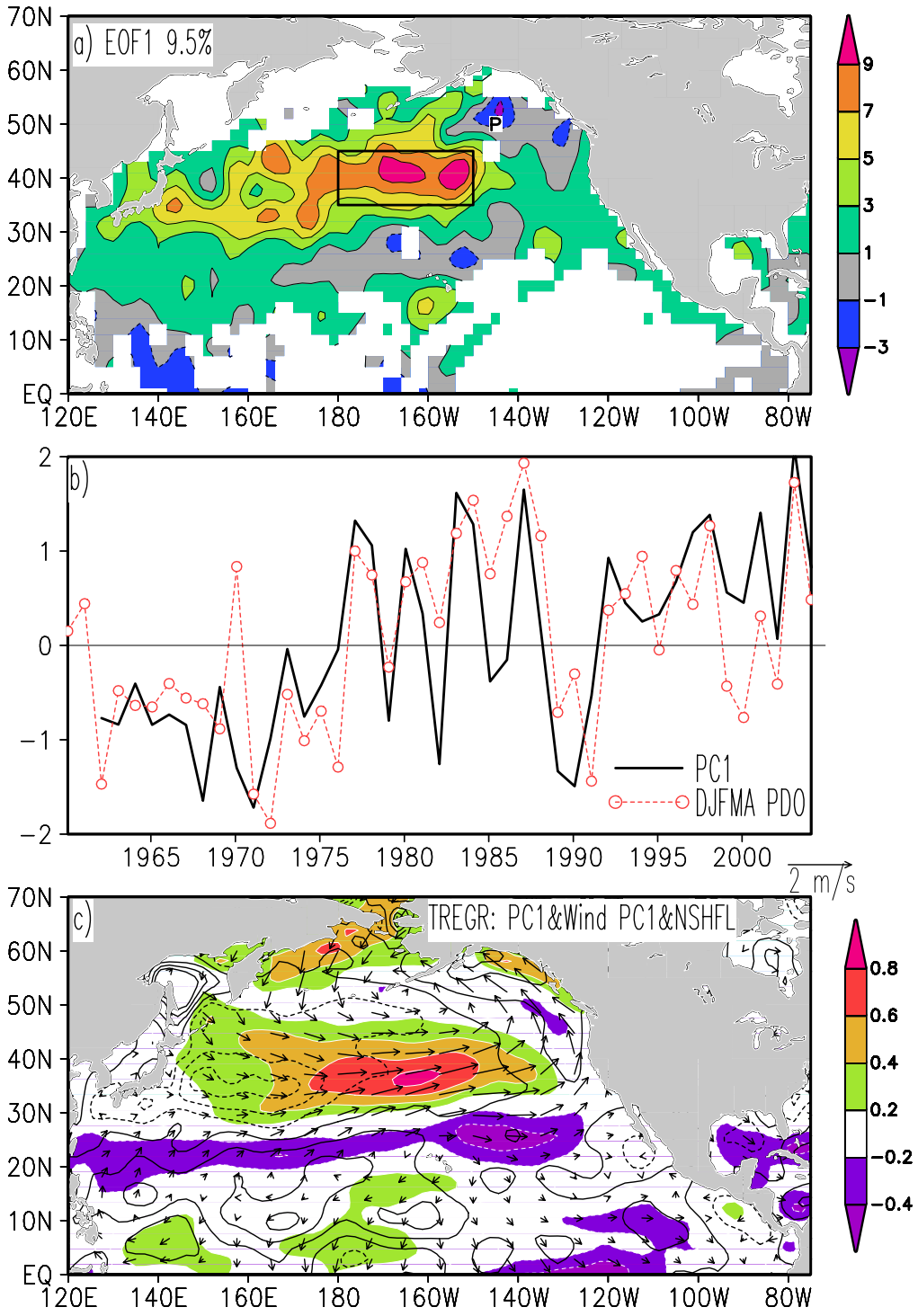

Figure 7 Climate variability in the North Pacific during the months December-April. (a) Spatial pattern of leading EOF of MLD. (b) Principal component time series and PDO Index time series of *Mantua et al. (1997)*. (c) Projection of anomaly vector winds, wind speed (shading), and the net surface heat flux (contours interval 5 Wm^{-2}, negative - dashed) on the principal component time series. Location of station Papa is indicated in (a) as "P".

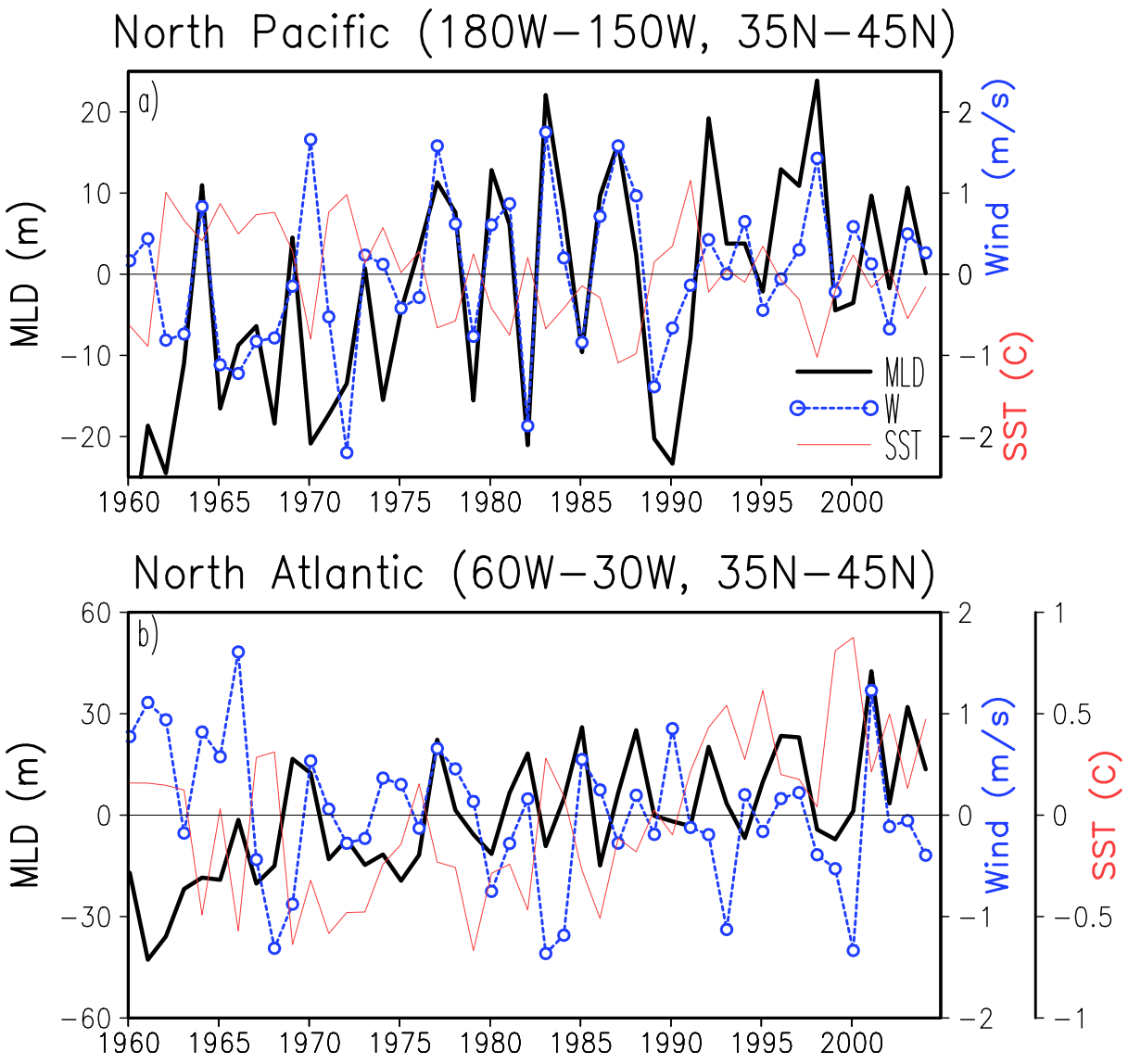

Figure 8 December-April anomalies averaged (a) across the central North Pacific box (defined in **Fig. 7**) and (b) across the central North Atlantic box (defined below in **Fig. 9**). The scale for mixed layer depth is shown on left (m), while scales for SST (^{o}C) and winds (ms^{-1}) are shown on right. In the Pacific the correlation between anomalous MLD and wind speed is r=0.61, while the correlation between anomalous MLD and SST is r=-0.48. In the Atlantic at decadal periods MLD and SST both show increasing trends.

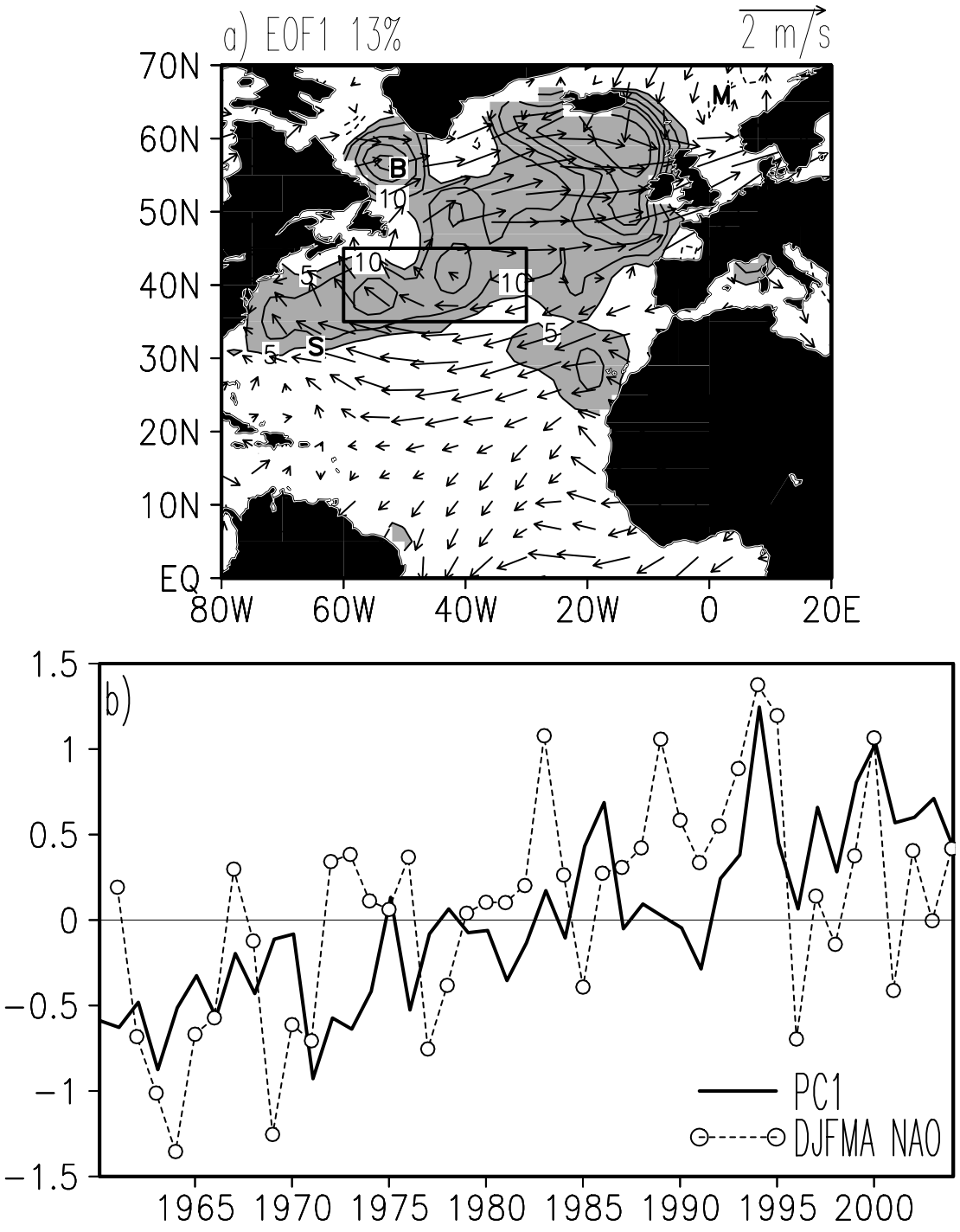

Figure 9 Climate variability in the North Atlantic during the months December-April (a) Spatial pattern of leading Empirical Orthogonal Eigenfunction of MLD. Projection of December-April winds on the principal component time series is overlain. (b) Principal component time series and the NAO index of *Barnston and Livezey* (1987). Locations of stations Bravo, M, and S are shown in (a) with corresponding letters.

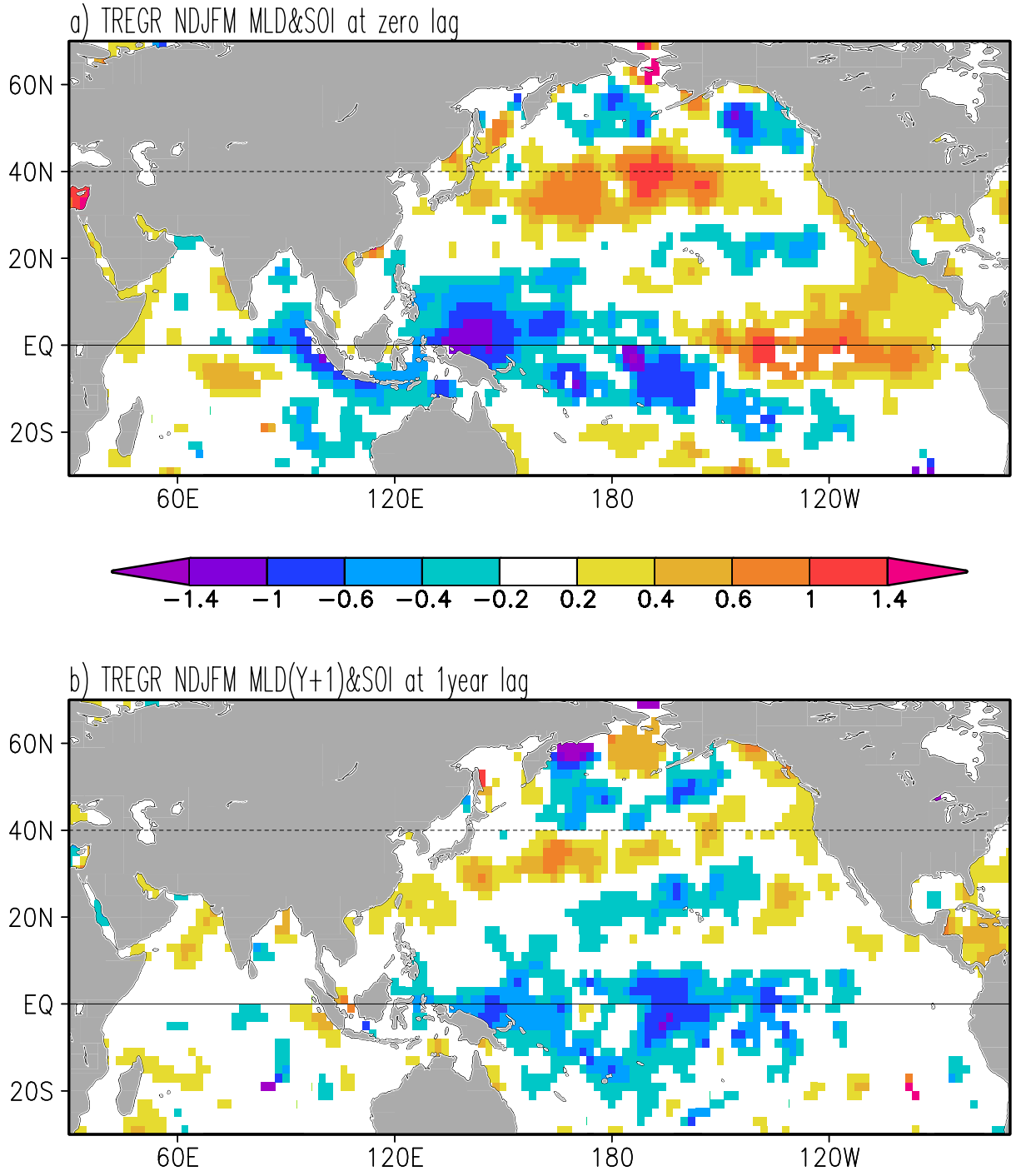

Figure 10 Time regression (a) of the November-March anomaly MLD and the reversed sign SOI index in the Indian and Pacific sectors. (b) lagged regression of for the next November-March anomaly MLD(Y+1) and –SOI(Y+0). Units are m/(unit SOI).

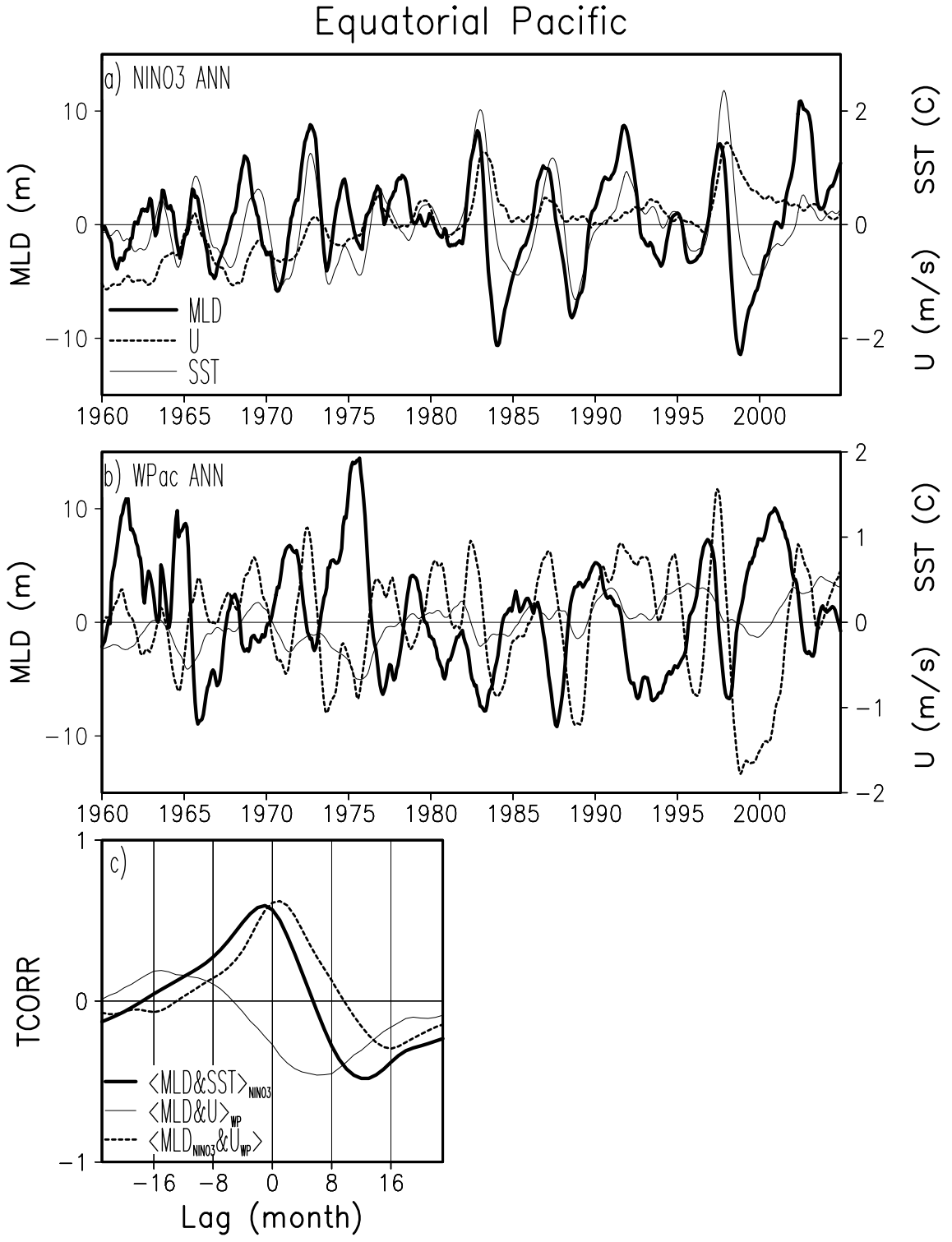

Figure 11 One year running mean anomaly MLD, SST, and zonal wind (*U*) (a) in the NIÑO3 box (210°-270°E, 5°S-5°N), (b) in a western Pacific box (135°-180°E, 5°S-5°N). (c) Lag correlation among *monthly averaged* NIÑO3 and western Pacific variables. Positive lags imply that the second variable leads the first.

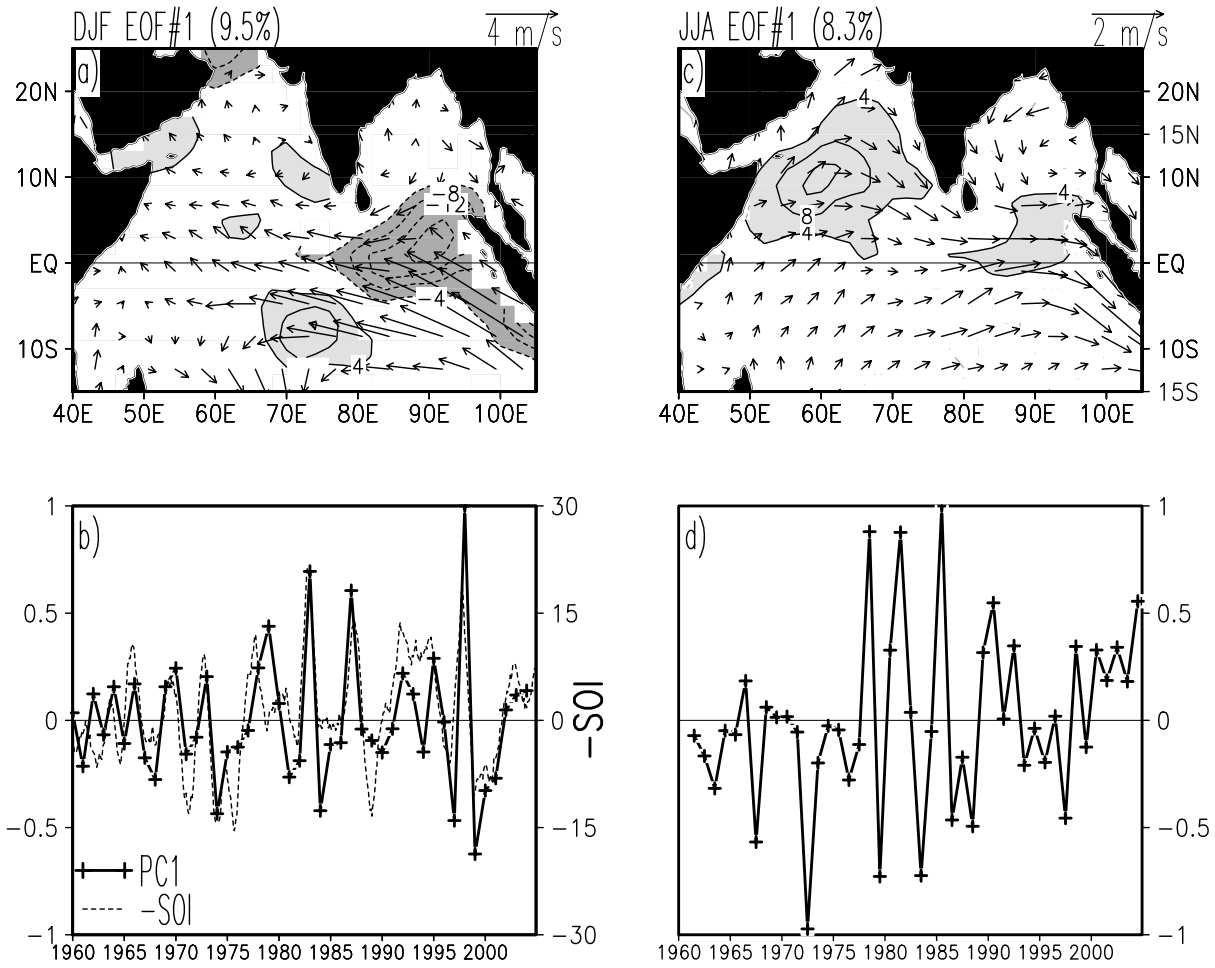

Figure 12 Variability in the Indian Ocean sector during (left)the season of the mature phase of ENSO SSTs (DJF) and (right) during the season of the Southwest Monsoon (JJA). **(**a,c) Spatial patterns of leading Empirical Orthogonal Eigenfunction of MLD; Time regression of winds onto the EOF time series is overlain. (b,d) Corresponding principal component time series (solid). The SOI index for DJF is overlain in (b). Correlation of PC1 and -SOI time series is 0.75.